

Friction in Granular Layers: Hysteresis and Precursors

S. Nasuno,* A. Kudrolli, and J. P. Gollub†

Physics Department, Haverford College, Haverford, Pennsylvania 19041
and Department of Physics, University of Pennsylvania, Philadelphia, Pennsylvania 19104

(Received 9 April 1997)

Sensitive and fast force measurements are performed on sheared granular layers with simultaneous optical imaging. Discrete displacements that can be much smaller than the particle diameter occur for low imposed velocity gradients, with a transition to continuous motion at a higher gradient. The instantaneous frictional force measured within individual slip events is a multivalued function of the instantaneous velocity. Localized microscopic rearrangements precede (and follow) macroscopic slip events; the accumulation of localized rearrangements leads to macroscopic creep. [S0031-9007(97)03732-0]

PACS numbers: 83.70.Fn, 47.55.Kf, 62.40.+i, 81.05.Rm

The response of a granular medium to shear forces is important both as a fundamental physical property of these materials [1,2] and for understanding earthquake dynamics [3,4], where slipping events occur along faults that are often separated by a granular “gouge.” Stick-slip motion often occurs at low shear or strain rates; its occurrence can be explained phenomenologically by a friction law that declines with velocity v , and a stiffness (see below) that is less than a critical value [5]. A molecular dynamics simulation of granular friction [6] suggests that repetitive shear-induced fluidization accompanies stick-slip motion. Though models exist for steady state forces [7], the actual time-dependent frictional force during individual slip events appears not to have been measured or computed for granular materials. Previous measurements [8–12] of frictional forces in sheared granular media have mostly emphasized large systems, high velocity flows, and large normal stresses, in contrast to those reported here, which also allow direct imaging of the particle dynamics.

In this Letter, we report sensitive measurements of frictional forces produced by sheared layers of polydisperse particles, with simultaneous optical imaging to reveal microscopic particle displacements. We are able to determine the force variations *within slip events lasting as little as 40 ms*. We find $F_f(v)$ to be multivalued, with the instantaneous force being less for decreasing than for increasing velocities. This hysteresis, which occurs in conjunction with a slight dilation of the material, is important in understanding the observed dynamics.

Very slow displacement (creep) is known to precede the rapid slip events [4,13–15], but its microscopic mechanism remains unclear, and may be quite different for granular materials than for solid-on-solid friction. In the present work, we find that significant microscopic rearrangement events occur during the sticking intervals. Their accumulation leads to creep, and their frequency rises dramatically as the slips are approached. Similar patterns are known in connection with earthquakes [16,17]. We also study the effects of various system pa-

rameters on the dynamics, and we show that, in some cases, the stick-slip dynamics can be nonperiodic and the discrete displacements surprisingly small.

Apparatus—A schematic diagram of our experimental setup is shown in Fig. 1. The granular layer typically consists of spherical glass beads whose size distribution includes particles 70–110 μm in diameter. Shear stress is applied by pushing a transparent glass cover plate with a leaf spring of adjustable stiffness and a stainless steel ball bearing coupler glued to the cover plate. The spring mount is attached to a translating stage whose micrometer is driven by a computer-controlled stepping motor. The translator moves at a pushing speed V , while the cover plate moves at speed $\dot{x}(t) \equiv v(t)$. The relative position $\delta x(t) = Vt - x(t)$ of the cover plate (relative to the spring mount) is determined to within 0.1 μm , using inductive displacement sensors similar to those used in Ref. [14]. This signal is equal to the spring deflection and is hence proportional to the spring force applied to the plate. We also monitor the vertical displacement of the cover plate with a separate inductive sensor.

The main part of the apparatus is mounted on a microscope, which allows the observation of microscopic motion of granular particles through the transparent top plate. The particle motion can be captured on video tape for

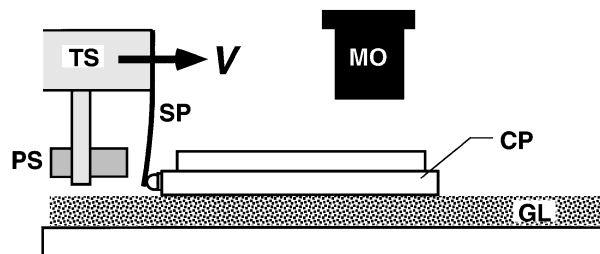


FIG. 1. Schematic diagram of the apparatus, showing the granular layer (GL) and a transparent cover plate (CP) pushed by a leaf spring (SP) connected to a translating stage (TS). An inductive sensor (PS) detects the deflection of the leaf spring. The microscope objective (MO) is also shown.

later quantitative analysis, or digitized directly. Synchronization allows events in the images to be correlated with structure in the force measurements. The apparatus and microscope are contained within a temperature controlled box and maintained somewhat above room temperature (37.5 ± 0.2 °C) and at a reduced humidity ($20\% \pm 2\%$) to minimize absorbed water on the particles. We typically use a layer thickness of 2 mm, which is uniform to about $50 \mu\text{m}$ initially. For our samples, cohesive forces are negligible.

The horizontal dimensions of the upper plate are generally 75×50 mm; the lower one is much larger. The surfaces of the plates can be treated in several ways to transmit the shear force to the granular layer without interfacial slipping. We roughen the bottom plate and either (a) glue a layer of particles to a glass top plate, or (b) rule a Plexiglas top plate with parallel grooves, 2 mm apart, so that imaging measurements can be made in the interstices. Similar results are found in the two cases. Particles are used only for a few runs to avoid the effects of wear.

Detailed studies reported here utilized the following ranges of the major parameters: imposed translation or pushing velocity V of the spring mount (10^0 – $10^4 \mu\text{m/s}$); layer thickness (2 mm); spring constant k (10^2 – 10^4 N/m); mass M of the upper plate (1 – 5×10^{-2} kg). Edge effects (due to the finite horizontal size of the layer) are believed to be negligible. Limited experiments were also performed on hollow ceramic beads, whose surfaces are rough, and on clean filtered sand.

Stick-slip phenomena.—For relatively low V , the top plate alternately sticks and slips (Fig. 2). During the static intervals, the top plate is at rest, and the spring deflection δx increases linearly in time [Fig. 2(a)] up to a maximum value corresponding to the maximum static friction force F_s . When this value is reached, the granular layer can no longer sustain the imposed shear stress, and the plate suddenly accelerates, while the friction force F_f decreases. When the imposed stress becomes

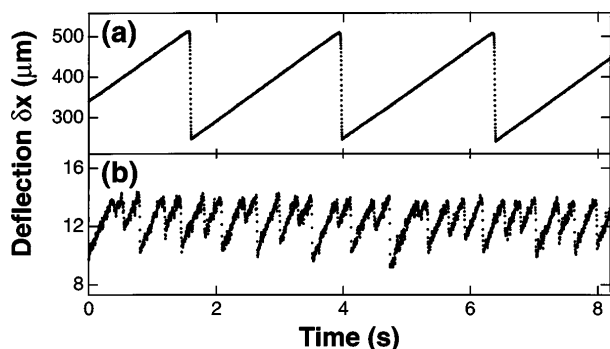


FIG. 2. (a) Spring deflection $\delta x(t)$ as a function of time for periodic stick-slip motion at pushing speed $V = 113.33 \mu\text{m/s}$, spring constant $k = 135$ N/m, and mass $M = 1.09 \times 10^{-2}$ kg. (b) Irregular stick-slip motion at $V = 11.33 \mu\text{m/s}$ and $k = 3636$ N/m.

sufficiently small, sticking recurs. The slip duration τ_s is comparable to the characteristic inertial time $\tau_{\text{in}} = 2\pi\sqrt{M/k}$ and is substantially shorter than the time between slip events. The granular flow during slip seems to occur predominantly in the top few layers of particles. Visual observation through the top plate reveals that the onset of sliding involves fluidization of granular particles in the upper layers. Measurement of *vertical* displacement confirms that the layer thickness increases by roughly $15 \mu\text{m}$ during the slip events, which is less than the mean particle diameter.

The observed stick-slip motion is almost periodic for a wide range of parameter values. However, strongly nonperiodic motion occurs at very low V and large k , as shown in Fig. 2(b). The mean period is short, and the displacement per cycle (about $2 \mu\text{m}$) is less than the particle diameter. Under these conditions, the maximum static force is almost the same for each cycle, but the degree to which the stress is unloaded (and hence the time of resticking) varies from cycle to cycle, probably because the degree of fluidization is low and many microscopic configurations are possible in a disordered medium.

As V increased, the mean period T decreases while the slip distance per event remains fairly constant, until an inertia-dominated regime is reached, where the oscillations of both the spring force and the frictional force are nearly (but not precisely) sinusoidal. Inertial effects in friction studies have been considered in Ref. [18]. A transition to continuous sliding (with fluctuations) occurs at a critical value V_c (6 mm/s for $k = 1077$ N/m and $M = 1.09 \times 10^{-2}$ kg). This threshold decreases with increasing k and also varies with M . The oscillation amplitude fluctuates strongly near V_c . A detailed study of the transition from inertial oscillation to continuous sliding will be published elsewhere [19].

We now consider the instantaneous velocity variations of the moving plate during individual slip events as shown in Fig. 3(a). It is remarkable that the behavior during slip for different V is nearly identical when k and M are fixed. The acceleration and deceleration portions of the pulse are different, and resticking is sudden. The maximum slip speed is of the order of F_s/\sqrt{km} and decreases with increasing k .

Frictional force.—We have determined the instantaneous normalized frictional force $\mu(t) = F_f(t)/Mg$ during the slip events. This quantity is derived from the measured force data by first obtaining the position $x(t)$ and the acceleration $\ddot{x}(t)$ of the top plate from the measured displacement signal $\delta x(t) = Vt - x(t)$, and then using the force balance equation $M\ddot{x} = k\delta x - F_f$. In Fig. 3(b) we plot the instantaneous frictional force as a function of the instantaneous sliding velocity $v(t) = \dot{x}(t)$. During the sticking period, μ increases linearly in time from a to b . When μ reaches the static threshold $\mu_s = F_s/Mg$, the top plate starts to slide. During the acceleration phase b to c , μ decreases monotonically from μ_s as the slip speed

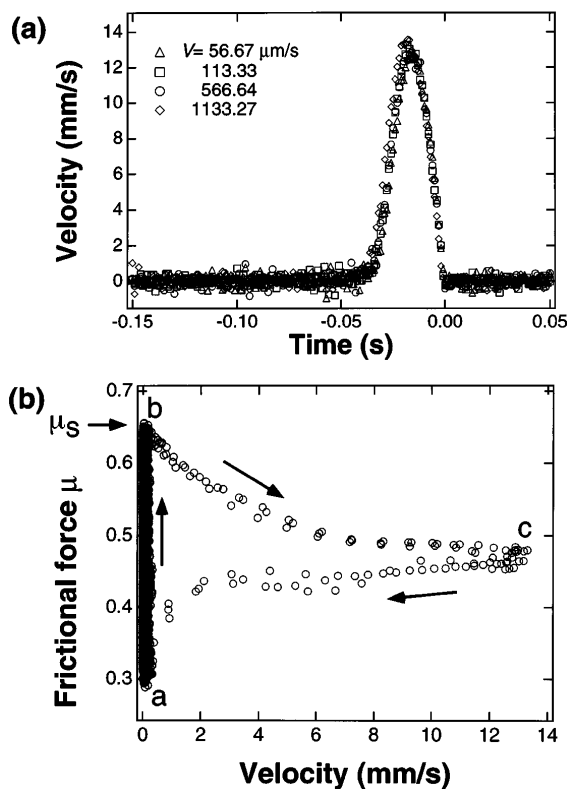


FIG. 3. (a) Instantaneous velocity $\nu(t)$ of the cover plate during slippage for various pushing speeds in the stick-slip regime ($k = 135 \text{ Nm}^{-1}$; $M = 1.09 \times 10^{-2} \text{ kg}$). The time origins of the pulses are forced to agree at the end of each event. (b) The instantaneous normalized frictional force $\mu(t) = F_f(t)/Mg$ as a function of $\nu(t)$, for three slip events at $V = 113 \mu\text{m/s}$.

increases. During the *deceleration* portion *c* to *a*, μ continues to decrease slowly at first and then rapidly as the slider comes to rest. This loop is almost identical for all events in a run.

The frictional force is not a single valued function of velocity; it is larger for increasing than for decreasing velocity within individual events. Delay or memory effects [20] also occur in solid-on-solid friction, but have a different origin. One source of delay here is the time (about 2 ms) required for the plate to fall a distance equal to the observed vertical dilation during the slip pulse (about $15 \mu\text{m}$). The force may possibly be modeled by introducing state variables in addition to $\nu(t)$, as is done in studies of rock friction; see Refs. [4,5].

Precursors.—Microscopic observations permit us to detect local particle motion within the granular layer. To allow optical access, we use a ruled Plexiglas plate, as discussed earlier. We find that local rearrangements of granular particles occur even during the sticking interval. These small motions can be detected by taking differences between successive images. We coarse grain the image over a size comparable to the particle diameter. Then the number of spots for which the difference image is nonzero

is a measure of the number of particles that have been displaced between the two images. An image of a portion of the layer (about 10 grains or 1 mm in width) is shown in Fig. 4, along with a sample difference image showing local displacements in 1 s. We find that the microscopic rearrangement rate, as indicated by the average number $\langle n(t) \rangle$ of microscopic displacement sites (in a 1 s interval and a 4 mm^2 area), increases rapidly near the time of a slip event, as shown in Fig. 5(a). The data has been averaged over 416 major slip events. Note that the event rate is asymmetric, with precursors being somewhat more likely than microscopic events at an equivalent time *after* a major slip occurs at $t/T = 0$.

The precursors are detectable macroscopically as well because they contribute to a small amount of creep before the major events. This creep process is shown in Fig. 5(b). The accumulated precursors produce a displacement about 1% as large as that occurring during a slip event. There is substantial variability from one event to the next; the probability distribution $P(N)$ of the *total* number N of macroscopic slip sites occurring at any time before or after a single major slip event is broad, approximately exponential, with a decay constant of about 40 events. The most likely explanation for the local rearrangement events is the breaking of chains of particles that sustain most of the stress [1,2,21].

In conclusion, within slip events, fluidization and dilation of the granular material cause the frictional force to decline with increasing instantaneous velocity, and the lower value is maintained for at least 10 ms even as $\nu(t)$ subsequently decreases. The measured dilation is small, much less than the particle size. We have also observed striking localized precursors and post-slip rearrangements, which are the microscopic origin of slow creep between slip events. It may be possible to determine by faster imaging whether some of the precursors grow spatially into macroscopic slip events. There is a need for improved phenomenological models that apply on the short time scales of individual slip events, and microscopic models that can explain the small slip

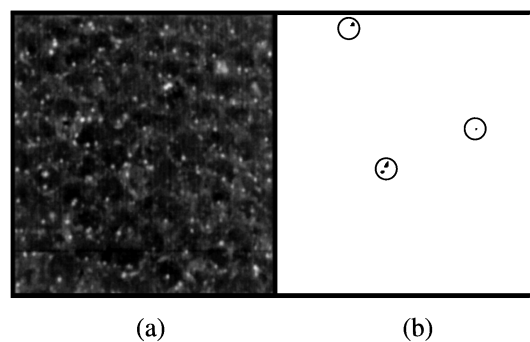


FIG. 4. (a) Image of a portion of a granular layer (about 1 mm across), and (b) difference image ($\Delta t = 1 \text{ s}$) showing localized particle rearrangements (circled) between major slip events.

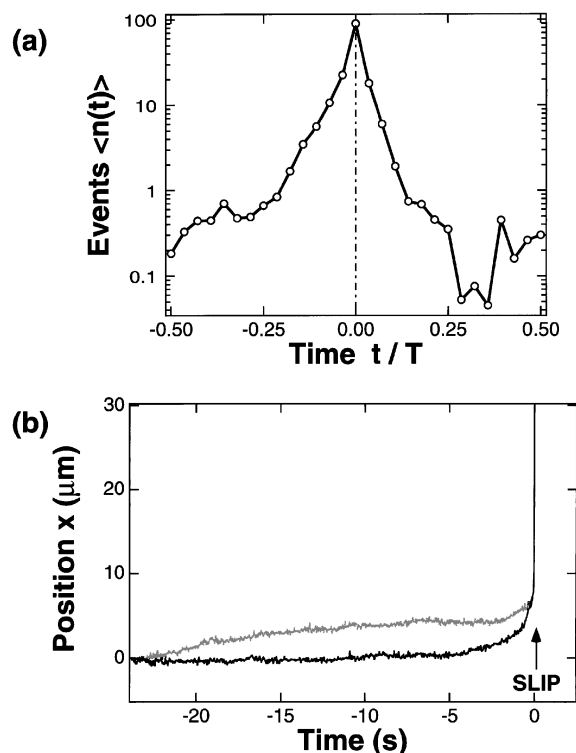


FIG. 5. (a) Average number of microscopic slip sites (per sec in a 4 mm^2 area) as a function of time before or after a major slip event, in units of the period T of the stick-slip cycle. (b) Displacement creep (of variable amount) before several major slip events.

displacements (much less than a particle diameter) that we noted for high stiffness. It is interesting to note that small irregular displacements also occur in thin lubricated films due to constrained dynamics [22].

We have varied many aspects of the experiments, including the translation velocity, spring constant, mass of the upper plate, and the mean size of the particles. The qualitative effects reported here are robust. A more detailed report, including studies of the inertial regime, the transition to continuous motion, and rough particles, will be published elsewhere [19]. Though these experiments are conducted at much lower normal stress than situations relevant to geophysics, they provide insight into the dynamics of sudden slip events, and about localized precursors.

This work was supported in part by the National Science Foundation Grant No. DMR 9319973. S.N. acknowledges the support of the Ministry of Education, Science, Sports, and Culture of Japan. We appreciate the assistance of Anthony Bak with some of the experiments,

and we thank P. Molnar, G. S. Grest, and J. M. Carlson for helpful suggestions.

*Permanent address: Department of Electrical Engineering, Kyushu Institute of Technology, Tobata, Kitakyushu 804, Japan.

Electronic address: nasuno@ele.kyutech.ac.jp

†To whom correspondence should be addressed.

Electronic address: jgollub@haverford.edu

- [1] H. Jaeger, S.R. Nagel, and R.P. Behringer, *Rev. Mod. Phys.* **68**, 1259 (1996).
- [2] B. Miller, C. O'Hern, and R.P. Behringer, *Phys. Rev. Lett.* **77**, 3110 (1996).
- [3] J.M. Carlson, J.S. Langer, and B.E. Shaw, *Rev. Mod. Phys.* **66**, 657 (1994).
- [4] C.H. Scholz, *The Mechanics of Earthquakes and Faulting* (Cambridge University Press, Cambridge, England, 1990).
- [5] A. Ruina, *J. Geophys. Res.* **88**, 10359 (1983).
- [6] P.A. Thompson and G.S. Grest, *Phys. Rev. Lett.* **67**, 1751 (1991).
- [7] H.M. Jaeger, C.H. Liu, S.R. Nagel, and T.A. Witten, *Europhys. Lett.* **11**, 619 (1990).
- [8] D.M. Hanes and D. Inman, *J. Fluid Mech.* **150**, 357 (1985).
- [9] D.R. Scott, C.J. Marone, and C.G. Sammis, *J. Geophys. Res.* **99**, 7231 (1994).
- [10] D.G. Wang and C.S. Campbell, *J. Fluid Mech.* **244**, 527 (1992).
- [11] S.B. Savage and M. Sayed, *J. Fluid Mech.* **142**, 391 (1984).
- [12] N.M. Beeler, T.E. Tullis, M.L. Blanpied, and J.D. Weeks, *J. Geophys. Res.* **101**, 8697 (1996).
- [13] J.H. Dietrich, *J. Geophys. Res.* **83**, 3940 (1978).
- [14] F. Heslot, T. Baumberger, B. Perrin, B. Caroli, and C. Caroli, *Phys. Rev. E* **49**, 4973 (1994).
- [15] T. Baumberger, F. Heslot, and B. Perrin, *Nature (London)* **367**, 544 (1994).
- [16] L.M. Jones and P. Molnar, *J. Geophys. Res.* **84**, 3596 (1979).
- [17] B.E. Shaw, J.M. Carlson, and J.S. Langer, *J. Geophys. Res.* **97**, 479 (1992).
- [18] J.R. Rice and S.T. Tse, *J. Geophys. Res.* **91**, 521 (1986).
- [19] S. Nasuno, A. Bak, A. Kudrolli, and J.P. Gollub, *Time-Resolved Studies of Stick-Slip Friction in Sheared Granular Layers* (to be published).
- [20] J.A.C. Martins, J.T. Oden, and F.M.F. Simões, *Int. J. Eng. Sci.* **28**, 29 (1990).
- [21] C.G. Sammis and S.J. Steacy, *Pure Appl. Geophys.* **142**, 777 (1994).
- [22] A. Demirel and S. Granick, *Phys. Rev. Lett.* **77**, 4330 (1996).